

Broad-band X-ray measurements of GS 1826-238

J.J.M. in 't Zand¹, J. Heise¹, E. Kuulkers^{1,2}, A. Bazzano³, M. Cocchi³, and P. Ubertini³

¹ Space Research Organization Netherlands, Sorbonnelaan 2, 3584 CA Utrecht, The Netherlands

² Astronomical Institute, Utrecht University, P.O. Box 80000, 3508 TA Utrecht, The Netherlands

³ Istituto di Astrofisica Spaziale (CNR), Area Ricerca Roma Tor Vergata, Via del Fosso del Cavaliere, I-00133 Roma, Italy

Received 12 February 1999 / Accepted 6 April 1999

Abstract. The broad band X-ray spectrum of the low-mass X-ray binary (LMXB) GS 1826-238 was measured with the narrow-field instruments on *BeppoSAX* on April 6 and 7, 1997. The spectrum is consistent with the Comptonization of a 0.6 keV thermal spectrum by a hot cloud of temperature equivalent $kT = 20$ keV. During the observation two type I X-ray bursts were detected. From the bursts an upper limit to the distance could be derived of 8 kpc. Combined with an elsewhere determined lower limit of 4 kpc this implies a persistent X-ray luminosity between 3.5×10^{36} and 1.4×10^{37} erg s⁻¹ which is fairly typical for a LMXB X-ray burster. The accurate determination of the energetics of the two bursts and the persistent emission confirm results with the Wide Field Cameras on *BeppoSAX* in a narrower bandpass (Ubertini et al. 1999). Comparison with independent X-ray measurements taken at other times indicates that GS 1826-238 since its turn-on in 1988 is a rather stable accretor, which is in line with the strong regularity of type I X-ray bursts.

Key words: stars: individual: GS 1826-238 – stars: neutron – X-rays: bursts – X-rays: stars

1. Introduction

A decade after its discovery (Makino et al. 1989), the nature of the compact object in the X-ray binary GS 1826-238 has finally been established. Monitoring observations with the Wide Field Cameras (WFCs) on *BeppoSAX* revealed the source to be a regular source of type I X-ray bursts which are explained as thermonuclear runaway processes on the hard surface of a neutron star (Ubertini et al. 1997, 1999). Previously, the nature was under debate because the X-ray emission exhibited characteristics that were until recently suspected to be solely due to black hole candidates (Tanaka 1989).

An optical counterpart has been identified (Motch et al. 1994, Barret et al. 1995) which classifies the binary as a low-mass X-ray binary (LMXB). Later this counterpart was found to exhibit optical bursts and a modulation which is likely to have a periodicity of 2.1 h (Homer et al. 1998). If the latter is

interpreted to be of orbital origin, it would imply a binary that is compact among LMXBs.

GS 1826-238 appears unusual among LMXBs. First, X-ray flux measurements after its 1989 discovery are fairly constant (In 't Zand 1992, Barret et al. 1995) at a level of approximately 6×10^{-10} erg cm⁻² s⁻¹ in 2 to 10 keV. Second, the WFC measurements reveal a strong regularity in the occurrence of type I X-ray bursts for an unusually long time (Ubertini et al. 1999). These two facts are very probably related. The constant flux is indicative of a stable accretion of matter on the neutron star which fuels regularly ignited thermonuclear explosions that give rise to X-ray bursts.

GS 1826-238 has a hard spectrum, the initial *Ginga* observations measured a power law spectrum with a photon index of 1.8 (Tanaka 1989). This makes it particularly important to study the spectrum in a broad photon energy range. Strickman et al. (1996) have attempted this by combining the early *Ginga* 1–40 keV data with 60–300 keV OSSE data taken in 1994. Del Sordo et al. (1998) have performed a preliminary study of the 0.1–100 keV data taken with the narrow-field instruments (NFI) on board *BeppoSAX* in October 1997. In the present paper, we study data taken with the same instrumentation half a year before that. The primary purpose of this study is to accurately analyze the flux of the persistent emission as well as that of two X-ray bursts. Also, we study the variability of the 2 to 10 keV emission.

2. Observations

The NFI include the Low-Energy and the Medium-Energy Concentrator Spectrometer (LECS and MECS, see Parmar et al. 1997 and Boella et al. 1997 respectively) with effective bandpasses of 0.1–10 and 1.8–10 keV, respectively. Both are imaging instruments. The MECS was used in the complete configuration of three units (unit 1 failed one month after the present observation). The other two NFI are the Phoswich Detector System (PDS; active between ~ 12 and 300 keV; Frontera et al. 1997) and the High-Pressure Gas Scintillation Proportional Counter (HP-GSPC; active between 4 and 120 keV; Manzo et al. 1997).

A target-of-opportunity observation (TOO) was performed with the NFI between April 6.7 and 7.2, 1997 UT (i.e., 40.8 ks time span). The trigger for the TOO was the first recognition

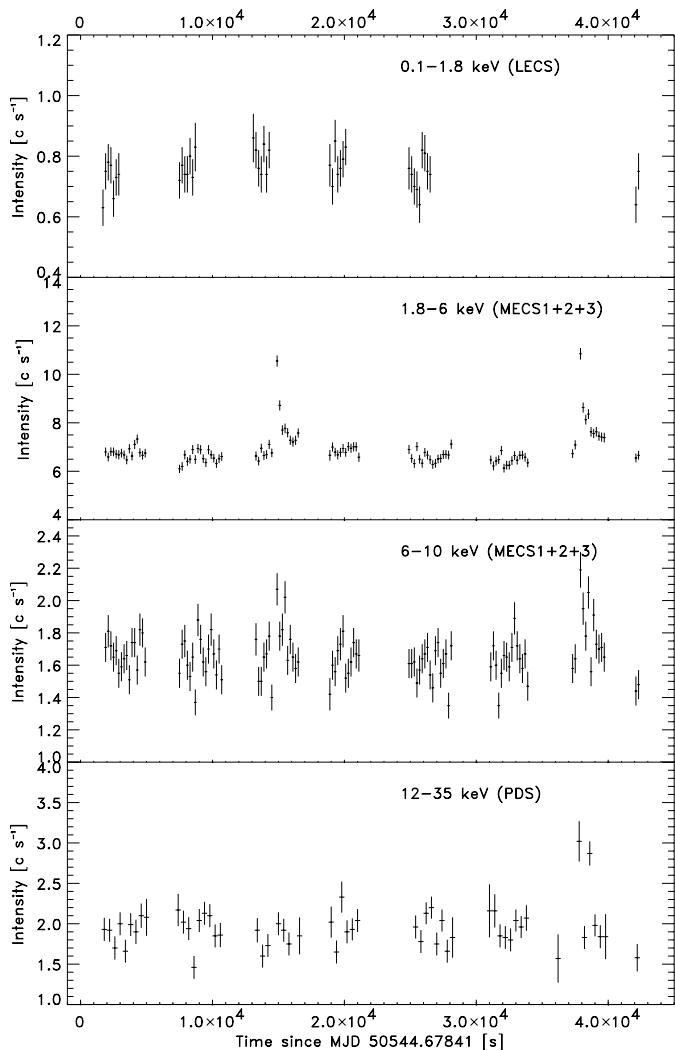


Fig. 1. Light curves of GS 1826-238 persistent emission. Background contributions have been subtracted. The data during the burst time intervals from -7 to $+113$ s with respect to the burst peak times have been excluded (see Figs 4 and 5). The time resolution is 200 s for the LECS and MECS data and 400 s for the PDS data.

that the source was bursting (Ubertini et al. 1997). The net exposure times are 8.2 ks for LECS, 23.1 ks for MECS, 18.0 ks for HP-GSPC and 20.5 ks for PDS. GS 1826-238 was strongly detected in all instruments and two ~ 150 s long X-ray bursts were observed.

We applied extraction radii of $8'$ and $4'$ for photons from LECS and MECS images, encircling at least $\sim 95\%$ of the power of the instrumental point spread function, to obtain lightcurves and spectra. Long archival exposures on empty sky fields were used to define the background in the same extraction regions. These are standard data sets made available especially for the purpose of background determination. All spectra are rebinned so as to sample the spectral full-width at half-maximum resolution by three bins and to accumulate at least 20 photons per bin. The latter will ensure the applicability of χ^2 fitting procedures. A systematic error of 1% is added to each channel of the

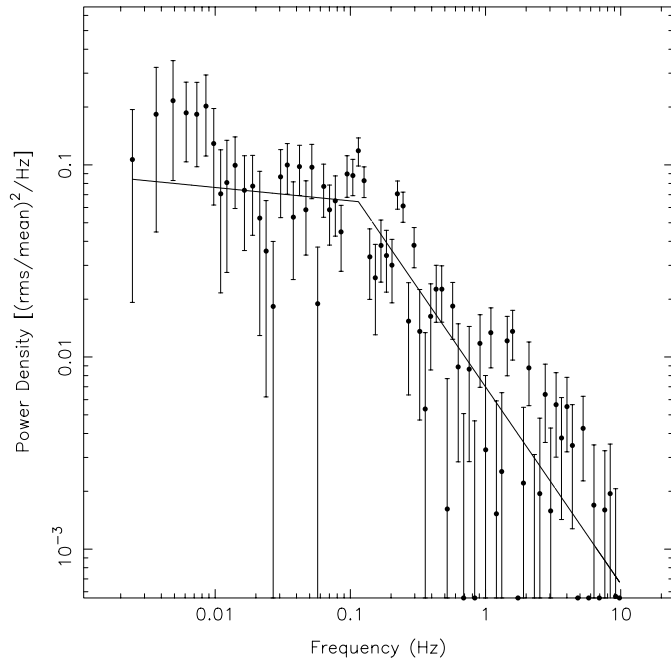


Fig. 2. Fourier power density spectrum of the intensity time series as measured with MECS between 2 and 10 keV. This is the average of the power spectra of 31 time intervals of 819.2 s each with a time resolution of 0.05 s. The Nyquist frequency is 10 Hz and the original frequency resolution $1/819.2$ Hz. The frequency domain was logarithmically rebinned. The drawn line shows a broken power law function fitted to the data.

rebbinned LECS and MECS spectra, to account for residual systematic uncertainties in the detector calibrations (e.g., Guainazzi et al. 1998). For spectral analyses, the bandpasses were limited to 0.1–4.0 keV (LECS), 2.2–10.5 keV (MECS), 4.0–30.0 keV (HP-GSPC) and 15–200 keV (PDS) to avoid photon energies where the spectral calibration of the instruments is not yet complete. In spectral modeling, an allowance was made to leave free the relative normalization of the spectra from LECS, PDS and HP-GSPC to that of the MECS spectrum, to accommodate cross-calibration uncertainties in this respect. Use was made of the publicly available response matrices (version September 1997).

3. The persistent emission

Fig. 1 shows the lightcurve of the persistent emission of GS 1826-238 in various bandpasses. On time scales of a few hundred seconds, the flux appears constant except for immediately after the occurrence of the two bursts. We searched for a modulation on time scales of about 2.1 h in the MECS data (which are the most sensitive) and find none. The 3σ upper limit on the semi amplitude is 1.6%. Thus, we cannot, in X-rays, confirm the optical modulation which had a semi amplitude of 6%. The power spectrum of the same data (excluding the burst intervals) is shown in Fig. 2. A broken power law function was fitted to these data. The Poisson level, which is a free parameter, has been subtracted in Fig. 2. Formally, the fit is unacceptable

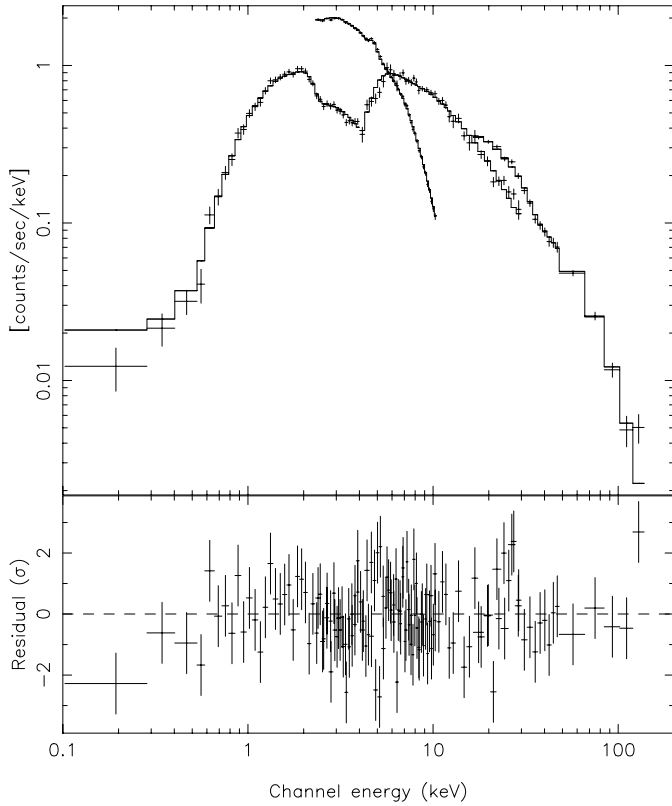


Fig. 3. *Upper panel:* count rate spectrum (crosses) and Comptonized spectrum model (histogram) for average persistent emission (excluding $-7/+1113$ s time intervals around the burst peaks). *Lower panel:* residual in units of σ per channel.

($\chi^2 = 134$ for 72 dof). This may be due to narrow features at 0.2–0.3 Hz and 1–2 Hz but the statistical quality of the data do not allow a detailed study of those. The break frequency of the broken power law is 0.115 ± 0.011 Hz, the power law index is -0.07 ± 0.10 below and -1.02 ± 0.12 above the break frequency. The high-frequency index is consistent with the index found from *Ginga* data taken in 1988 between 0.1 and 500 Hz (Tanaka 1989). The integrated rms power of the noise between 0.002 and 10 Hz is $20 \pm 2\%$, that for the *Ginga* data between 0.02 and 500 Hz is $\sim 30\%$ (Barret et al. 1995). If one assumes the same break frequency for the *Ginga* data, we expect an rms of 17% for these between 0.002 and 10 Hz which is very similar to the MECS result. The break frequency is comparable with values found for LMXB atoll sources and is one order of magnitude below values found for the bright LMXB Z sources (see Wijnands & Van der Klis 1999). We are unable to assess the history or variability of the low-frequency index or break frequency.

A broad-band spectrum was accumulated, averaged over the complete observation except the burst intervals, making use of the LECS, MECS, HP-GSPC, and PDS data. The spectrum was fitted with two models: black body radiation with unsaturated Comptonization (Titarchuk 1994), this is a model which is rather successful in describing other low-luminosity LMXBs as well (e.g., Guainazzi et al. 1998, In 't Zand et al. 1999); and black

Table 1. Parameter values of two spectral models fitted to the persistent emission. The errors are single parameter 1σ errors.

Model	Comptonized spectrum plus black body (<i>XSPEC: wa constant bb comptt</i>)
N_{H}	$(1.1 \pm 0.2) \times 10^{21} \text{ cm}^{-2}$
bb kT	$3.78 \pm 0.32 \text{ keV}$
bb R	$0.21 \pm 0.03 d_{10 \text{ kpc}} \text{ km}$
Wien kT_{W}	$0.581 \pm 0.010 \text{ keV}$
Plasma kT_{e}	$20.4 \pm 1.1 \text{ keV}$
Plasma optical depth τ	2.13 ± 0.10 for disk geometry 4.95 ± 0.21 for spherical geometry
Comptonization parameter y	0.72 ± 0.07 for disk geometry 3.91 ± 0.33 for spherical geometry
χ^2_{r}	1.225 (132 dof)
Flux 2–10 keV	$5.42 \times 10^{-10} \text{ erg cm}^{-2} \text{ s}^{-1}$
Flux 0.1–200 keV	$1.93 \times 10^{-9} \text{ erg cm}^{-2} \text{ s}^{-1}$
Model	cut off power law plus black body (<i>XSPEC: wa constant bb cutoffpl</i>)
N_{H}	$(5.4 \pm 0.2) \times 10^{21} \text{ cm}^{-2}$
bb kT	$0.91 \pm 0.03 \text{ keV}$
bb R	$3.1 \pm 0.3 d_{10 \text{ kpc}} \text{ km}$
Photon index	1.38 ± 0.03
Cut off	$51.69 \pm 0.03 \text{ keV}$
χ^2_{r}	1.534 (137 dof)
Flux 2–10 keV	$5.41 \times 10^{-10} \text{ erg cm}^{-2} \text{ s}^{-1}$
Flux 0.1–200 keV	$2.00 \times 10^{-9} \text{ erg cm}^{-2} \text{ s}^{-1}$

body radiation plus a power law component with an exponential cut off, this model was used by Del Sordo et al. (1998) for NFI data below 100 keV on GS 1826-238. The results are given in Table 1, a graph is shown in Fig. 3 for the Comptonized model.

A power law fit to the 60–150 keV PDS data is acceptable ($\chi^2_{\text{r}} = 0.7$ for 4 dof) and reveals a photon index of 3.3 ± 0.4 which is close to that found for the 60–300 keV OSSE data by Strickman et al. (1996) of 3.1 ± 0.5 .

The average 0.1 to 200 keV flux is $f_{0.1-200 \text{ keV}} = (1.93 \pm 0.10) \times 10^{-9} \text{ erg cm}^{-2} \text{ s}^{-1}$.

We compare the results with those obtained by Del Sordo et al. (1998) on NFI data taken half a year later on the same source. Del Sordo et al. find for the black body temperature $0.94 \pm 0.05 \text{ keV}$, for the cut off energy $49 \pm 3 \text{ keV}$, for the power law index 1.34 ± 0.04 , and for $N_{\text{H}} \approx 4.6 \times 10^{21} \text{ cm}^{-2}$. These values are consistent with ours. Furthermore, Del Sordo et al. (1998) quote a 2 to 10 keV flux of $5.6 \times 10^{-10} \text{ erg cm}^{-2} \text{ s}^{-1}$ which is only $\sim 4\%$ larger than what we find. This indicates that the flux and spectrum of GS 1826-238 did not change substantially over half a year.

The optical counterpart is reported to exhibit $E_{B-V} = 0.4 \pm 0.1$ (Motch et al. 1994, Barret et al. 1995). Follows that $A_{\text{V}} = 1.2 \pm 0.3$ and $N_{\text{H}} = (2.2 \pm 0.5) \times 10^{21} \text{ cm}^{-2}$ (according to the conversion of A_{V} to N_{H} by Predehl & Schmitt 1995). An interpolation from the HI maps in Dickey & Lockman (1990) reveals the same value for N_{H} . This value is inconsistent with the values for the two models of the NFI-measured spectrum (Table 1). We tried to accommodate $2.2 \times 10^{21} \text{ cm}^{-2}$ with these

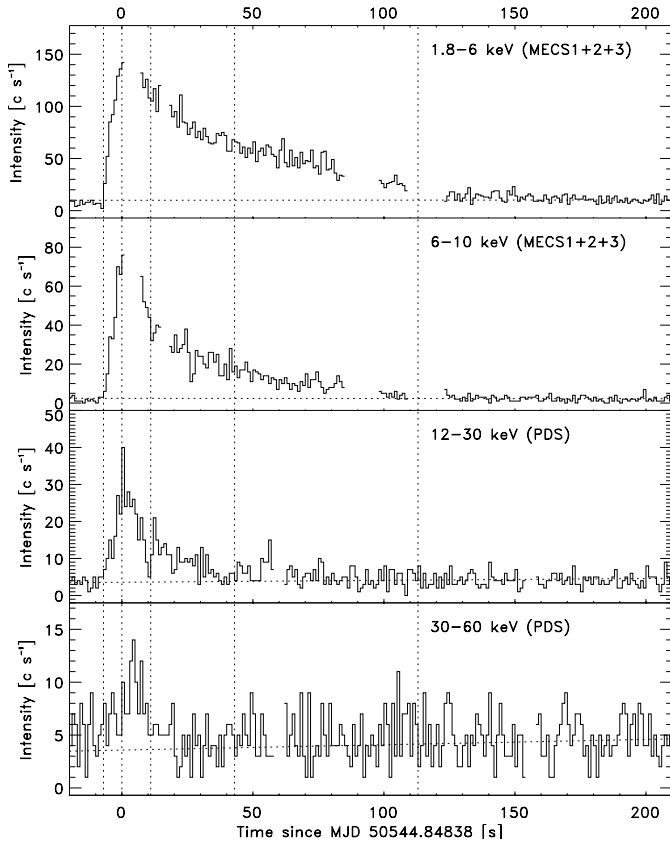


Fig. 4. Time profile of the first burst detected from GS 1826-238 with MECS and PDS. The time resolution is 1 s. The curves have not been corrected for contributions from the background and the persistent emission. The gaps in the MECS data correspond to times of bad data. The PDS curves were generated from collimator A and collimator B data, the gaps correspond to collimator slew times between off and on source position (these last 3 s and occur every 90 s). The linear trends as determined from the initial and final 10 s are drawn as near-horizontal dashed lines. The vertical lines indicate borders of time intervals for which spectra were modeled.

models. If N_{H} is frozen and the other parameters are left free, the Comptonized model remains a better description of the data with $\chi^2_{\text{r}} = 1.498$ (133 dof) than the black body plus cut-off power-law model with $\chi^2_{\text{r}} = 3.358$ (138 dof). The values of the other parameters in the Comptonized model are within the error margins as indicated in Table 1 except for kT_{W} which is marginally different at 0.496 ± 0.004 keV. Nevertheless, $\chi^2_{\text{r}} = 1.498$ is an unacceptable fit.

4. The burst emission

Figs. 4 and 5 show the time profiles of the two bursts in a number of bandpasses from MECS and PDS data at a time resolution of 1 s. There are no observations of the bursts with the LECS and we omit HP-GSPC data since this instrument has an energy range which overlaps that of the others. As far as can be judged (there are data gaps, probably due to telemetry overflow), the profiles are clean fast-rise exponential-decay shapes. The e-folding decay times per bandpass (see Table 2) are identical for

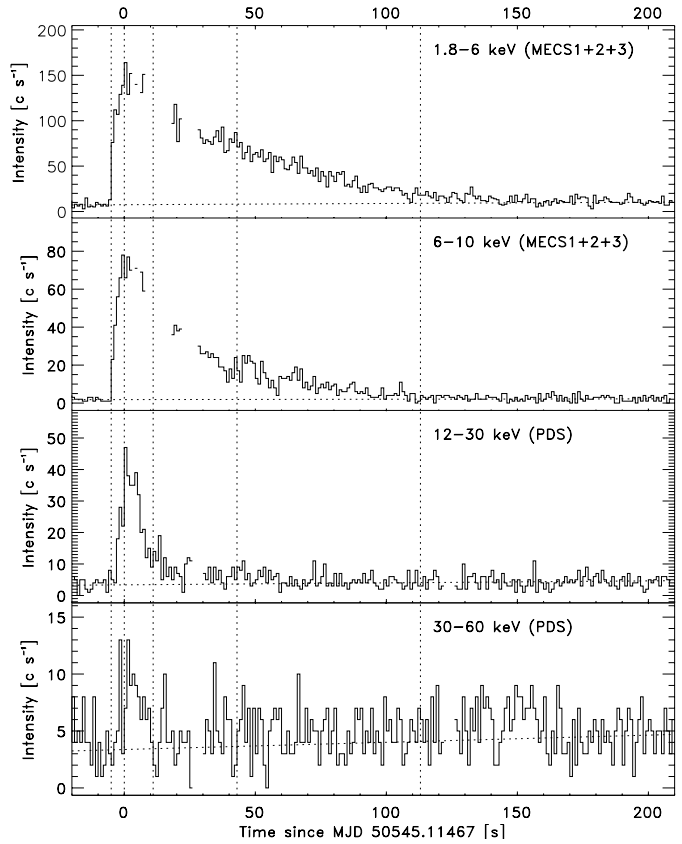


Fig. 5. Time profile of the second burst. For an explanation, see Fig. 4.

Table 2. Timing parameters and energetics of bursts

	burst 1	burst2
Peak time (MJD)	50544.84838	50545.11467
Decay time in 1.8–6 keV (s)	49.6 ± 1.2	49.2 ± 0.8
Decay time in 6–10 keV (s)	33.9 ± 1.3	34.1 ± 0.3
Bolometric fluence (10^{-7} erg cm^{-2})	8.1 ± 0.5	7.6 ± 0.5

both bursts. They are also long though not unprecedented, if compared to many other bursters. Furthermore, the rise time of the bursts is relatively large (5 to 8 s).

Each burst was divided in five time intervals (see Figs. 4 and 5). Relative to the peak time, the intervals are equal except for the first interval. The last interval of each burst covers 1000 s to study the slow decay of the flux to the persistent level. The persistent emission was not subtracted in these spectra while the background was. We fitted the MECS spectra in these intervals and in the non-burst data with a black body radiation model with different temperatures plus a power law function whose shape (i.e., photon index) is frozen over all intervals. Furthermore, a single level of interstellar plus circumstellar absorption was fitted to all data through N_{H} . PDS 15–30 keV data were included for the rise and first two decay time intervals of each bursts, as well as for the non-burst times up to 50 keV. The fit was reasonable with $\chi^2_{\text{r}} = 1.24$ for 470 dof. Results of the fit are given in Table 3. For illustrative purposes, a graph is presented

in Fig. 6 of the photon count rate spectra for 2 intervals of the second burst and the non-burst data.

This modeling of the burst spectral evolution shows that during the brightest parts of the bursts (between 0 and 113 s after the burst peaks) the black body radius remains constant within an error margin of roughly 10% while the temperature decreases from 2 to 1 keV. There is no evidence for photospheric expansion.

The photon count rate of the black body radiation in the PDS should be negligible above 30 keV (i.e., it is about 6×10^{-3} in 30–60 keV times that in 12 to 30 keV, for a black body with $kT = 2.2$ keV). However, as can be seen in Fig. 5, there is substantial burst emission between 30 and 60 keV. In fact, the average 30–60 keV photon count rate of the burst in the first 11 s after the burst peak is of order half times that in 12–30 keV. This suggests that the burst emission may be Comptonized like the persistent emission, although we are not able to verify that spectrally due to insufficient statistics.

5. Discussion

The thermal nature of the burst spectra with few keV temperatures and cooling are typical for a type I X-ray burst (e.g., Lewin et al. 1995, and references therein). Such a burst is thought to be due to a thermonuclear ignition of helium accumulated on the surface of a neutron star. The unabsorbed bolometric peak flux of the black body radiation is estimated at $(2.7 \pm 0.5) \times 10^{-8} \text{ erg cm}^{-2} \text{ s}^{-1}$. This translates into a peak luminosity of $(3.3 \pm 0.6) \times 10^{38} d_{10 \text{ kpc}}^2 \text{ erg s}^{-1}$. Since we do not find evidence for photospheric expansion in the bursts it is indicated that the burst peak luminosity is below the Eddington limit which is $1.8 \times 10^{38} \text{ erg s}^{-1}$ for a $1.4 M_{\odot}$ neutron star. Therefore, we expect the distance to be smaller than $7.4 \pm 0.7 \text{ kpc}$ or $\sim 8 \text{ kpc}$. Barret et al. (1995) infer from the photometry of the optical counterpart that the lower limit to the distance is 4 kpc. The relatively low galactic latitude of the source ($-6^{\circ}.1$) does not provide better constraints on the distance. For a distance between 4 to 8 kpc, the X-ray luminosity is between 3.5×10^{36} and $1.4 \times 10^{37} \text{ erg s}^{-1}$ which are fairly typical values for LMXB X-ray bursters.

The two bursts presented here show traces of Comptonization, like in X 1608–52 (Nakamura et al. 1989), 1E1724–308 in Terzan 2 (Guainazzi et al. 1998) and SAX J1748.9–2021 in NGC 6440 (In 't Zand et al. 1999). The PDS time profiles suggest that the level of Comptonization matches the burst quite closely. The time delay is less than a few seconds which suggests that the Comptonizing cloud is within $\sim 10^{11} \text{ cm}$. Unfortunately, this is not a strong constraint because a 2 h binary orbit implies a system size perhaps one order of magnitude smaller than that.

Many parameters of the two bursts are equal within narrow error margins: the durations within $0.8 \pm 2.8\%$, the peak temperatures within $7 \pm 3\%$, the peak emission areas within $2 \pm 5\%$, and the bolometric fluences within $6 \pm 6\%$. This suggests that the physical circumstances for triggering the bursts (i.e., the neutron star surface temperature and the composition of accreted matter) are the same on the two occasions and, together with

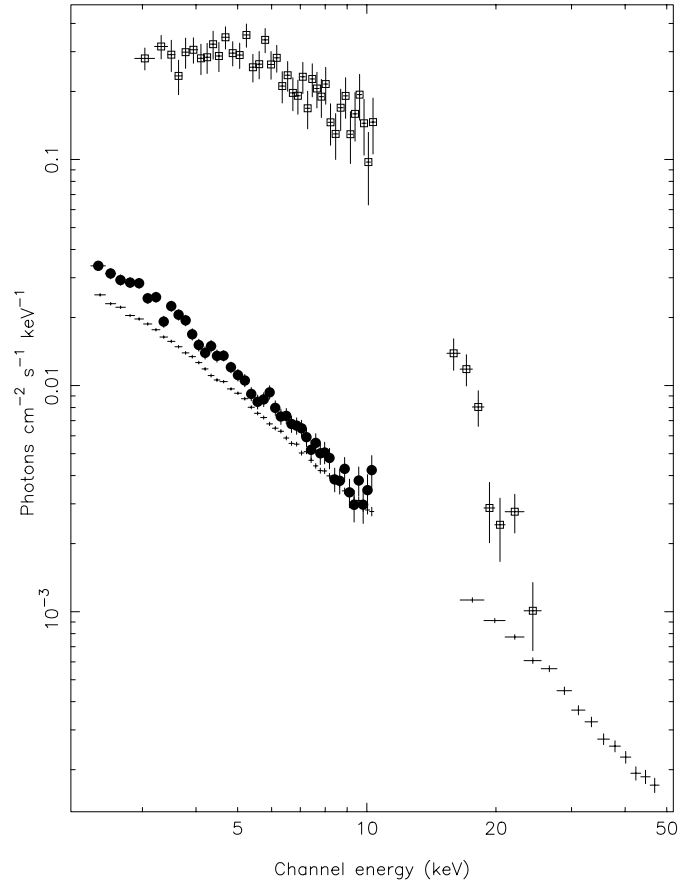


Fig. 6. From top to bottom, the photon spectrum of the 0/+11 s data of the second burst (rectangles), that of the +113/+1113 s data of the same burst (filled circles), and that of the non-burst data (no symbols, only error bars). Data are from MECS and PDS, except for the +113/+1113 s which is MECS only

the prolonged regular bursting and constant persistent flux as measured with WFC, testifies to a rather strong stability of the accretion process. This suggests a stable accretion disk. In how far this is uncommon among low-luminosity LMXBs remains to be seen. The knowledge about such LMXBs is as yet incomplete.

The broad-band spectral measurements of the persistent as well as burst emission enable a fairly accurate determination of α which is defined as the bolometric fluence of the persistent emission between two bursts and that of the latter burst. The time between the two bursts is 23,007 s. We are confident that no bursts were missed during the data gaps because this time is consistent with the quasi-periodicity of the burst recurrence as found from near-simultaneous WFC observations with period 5.8 hr and full-width at half maximum of 0.4 hrs (Ubertini et al. 1999). Of all 70 WFC-detected bursts from GS 1826-238, no two were closer to each other than 19,238 s. The fluence of the second burst is $(7.6 \pm 0.5) \times 10^{-7} \text{ erg cm}^{-2}$. The constant persistent emission implies a bolometric fluence between the two bursts of $(4.14 \pm 0.23) \times 10^{-5} \text{ erg cm}^{-2}$. Therefore, $\alpha =$

Table 3. Spectral parameters of two bursts. All data were simultaneously fitted, including the non-burst data.

	Time interval	-7/0 s ^a	0/11 s	11/43 s	43/113 s	113/1113 s
burst 1	bb kT (keV)	1.91 ± 0.06	1.96 ± 0.05	1.63 ± 0.03	1.33 ± 0.03	1.10 ± 0.06
	bb radius (km)	8.9 ± 0.5	10.9 ± 0.4	10.8 ± 0.4	10.4 ± 0.5	3.0 ± 0.3
	for $d_{10 \text{ kpc}} = 1$					
burst 2	bb kT (keV)	1.80 ± 0.08	2.11 ± 0.04	1.55 ± 0.04	1.36 ± 0.03	0.96 ± 0.05
	bb radius (km)	9.9 ± 0.8	10.7 ± 0.3	11.8 ± 0.5	9.5 ± 0.4	4.2 ± 0.4
	for $d_{10 \text{ kpc}} = 1$					

^a -5/0 s for the second burst

54 ± 5 . This confirms the value found from the WFC analysis (60 ± 7 , Ubertini et al. 1999).

Acknowledgements. We thank the *BeppoSAX* team at Nuova Telespazio (Rome) for planning and carrying out the observation presented here. *BeppoSAX* is a joint Italian and Dutch program.

References

- Barret D., Motch C., Pietsch W. 1995, *A&A* 303, 526
- Boella G., Chiappetti L., Conti G., et al. 1997, *A&AS* 122, 327
- Del Sordo S., Frontera F., Pdan E., et al. 1998, in Proc. 3rd Integral Workshop "The Extreme Universe", ed. A. Bazzano, Gordon & Breach, in press
- Dickey J.M., Lockman F.J. 1990, *ARA&A* 28, 215
- Frontera F., Costa E., Dal Fiume D., et al. 1997, *A&AS* 122, 357
- Guainazzi M., Parmar A.N., Segreto A., et al. 1998, *A&A* 339, 802
- Homer L., Charles P.A., O'Donoghue D. 1998, *MNRAS* 298, 497
- In 't Zand J.J.M. 1992, Ph.D. thesis, University of Utrecht
- In 't Zand J.J.M., Verbunt F., Strohmayer T.E., et al. 1999, *A&A* 345, 100
- Lewin W.H.G., Van Paradijs J., Taam R.E. 1995, in "X-ray Binaries", W.H.G. Lewin, J. van Paradijs, E.P.J. van den Heuvel (eds.), Cambridge University Press, Cambridge, p. 175
- Makino F. and the *Ginga* team 1989, *IAU Circ.* 4563
- Manzo G., Giarusso S., Santagelo A., et al., 1997, *A&AS* 122, 341
- Nakamura N., Dotani T., Inoue H., Mitsuda K., Tanaka Y. 1989, *PASJ* 41, 617
- Motch C., Barret D., Pietsch W., Giraud E. 1994, *IAU Circ.* 6101
- Parmar A.N., Martins D.D.E., Bavdaz M., et al. 1997, *A&AS* 122, 309
- Predehl P., Schmitt J.H.M.M. 1995, *A&A* 293, 889
- Strickman M., Skibo J., Purcell W., Barret D., Motch C. 1996, *A&ASS* 120, 217
- Tanaka Y. 1989, in "Proc. 23rd ESLAB Symposium on Two Topics in X-ray Astronomy", eds. J. Hunt & B. Battrick, ESA SP-296, p. 1
- Titarchuk L. 1994, *ApJ* 434, 313
- Ubertini P., Bazzano A., Cocchi M., et al. 1997, *IAU Circ.*, 6611
- Ubertini P., Bazzano A., Cocchi M., et al. 1999, *ApJ* 514, L27
- Wijnands R., van der Klis M. 1999, *ApJ* 514, 939